

Optoacoustic 3D visualization of changes in physiological properties of mouse tissues from live to postmortem

Richard Su, Sergey A. Ermilov, Anton V. Liopo, and
Alexander A. Oraevsky

TomoWave Laboratories Inc. 6550 Mapleridge St., Suite 124, Houston, TX 77081
www.tomowave.com

ABSTRACT

Using the method of 3D optoacoustic tomography, we studied changes in tissues of the whole body of nude mice as the changes manifested themselves from live to postmortem. The studies provided the necessary baseline for optoacoustic imaging of necrotizing tissue, acute and chronic hypoxia, and reperfusion. They also establish a new optoacoustic model of early postmortem conditions of the whole mouse body. Animals were scanned in a 37°C water bath using a three-dimensional optoacoustic tomography system previously shown to provide high contrast maps of vasculature and organs based on changes in the optical absorbance. The scans were performed right before, 5 minutes after, 2 hours and 1 day after a lethal injection of KCl. The near-infrared laser wavelength of 765 nm was used to evaluate physiological features of postmortem changes. Our data showed that optoacoustic imaging is well suited for visualization of both live and postmortem tissues. The images revealed changes of optical properties in mouse organs and tissues. Specifically, we observed improvements in contrast of the vascular network and organs after the death of the animal. We associated these with reduced optical scattering, loss of motion artifacts, and blood coagulation.

Keywords: photoacoustic thermoacoustic tomography, postmortem tissue changes, 3D tomography, nude mice, rigor mortis, blood coagulation, deoxygenation.

1. INTRODUCTION

Postmortem studies have a broad range of fields associated with it such as pathophysiological stages such as global changes of tissue in hypoxia and necrosis.^{1,2} It is important for forensic medicine, thermal therapy, and pathological anatomy. In the case of thermal therapy, it would be good to know when the targeted tissue is destroyed and how well the non-targeted tissue fair during the treatment. Another scenario is tissue hypoxia leading to necrosis like during frost bite when the blood circulation is restricted over a long span of time possibly killing the tissue.

It is known that the body undergoes various phases of changes during the time of necrosis in terms of physiology, chemistry, and biology of a specimen.^{3,4,5,6} Figure 1 shows many of the various transitions that the cells, tissues, and organs occur once the organism is dead. Physical changes happen rather quickly from minutes to days and consist of pallor (paleness), algor (temperature change), hypostasis (gravitation), etc. Also closely related to the physical changes are chemical changes which tend to also occur rather quickly ranging from minutes to weeks manifested in rigor mortis (cadaverous rigidity), blood coagulation, autolysis, etc. Biological changes like of putrefaction and further cadaverous decomposition related to bacteria and insects happen within days to months.^{7,8,9,10} Early changes associated with death include the loss of movement such as the fall of blood pressure and cessation of circulation of blood. Also the physical characteristics of the body such as temperature and rigidity happen in a span of a day. Within the first day following the death of an organism, changes to acoustic impedance and speed of sound are onset due to rigor mortis and blood coagulation in addition to deoxygenation which all can be detected with optoacoustic (OA) imaging.¹¹ Figure 2 presents some of the processes that lead to rigor mortis and blood coagulation due to the deoxygenation of the organism and subsequent creation of an acidic environment. This in turn causes contraction of the muscle fibers for rigor mortis and the release of thrombokinases when blood coagulation occurs. Upon rigor mortis, a dead organism previously flaccid for

two to three hours is becoming stiff starting from smaller muscle groups and proceeding to the whole body. This rigidity though is not permanent and begins to soften again after a day and a half to two days.

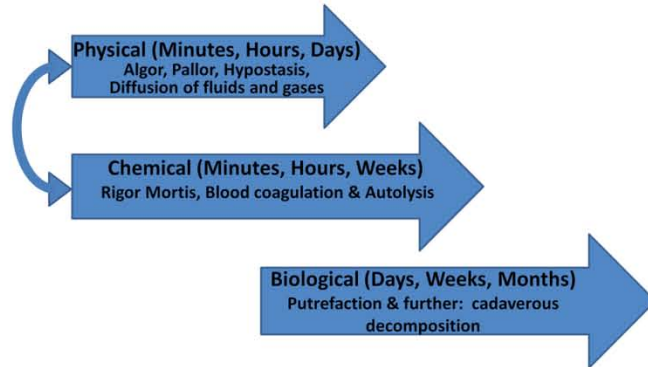


Figure 1. Diagram of various changes occurring within the body after death over time

Postmortem OA imaging has an advantage due to the loss of movement artifacts (breathing or muscle contractions during the scan). Rigor mortis, blood coagulation and loss of oxygen from the blood are the main events we attempt to see using OA imaging during early postmortem stages. It is known that prior to 800nm, deoxygenated blood is more optically absorbing than the oxygenated blood.¹² Additionally, there have been publications showing increased absorption and scattering of blood after photocoagulation.¹³ It was therefore hypothesized that optoacoustic imaging can track those acoustic and optical changes in terms of increased contrast over time.

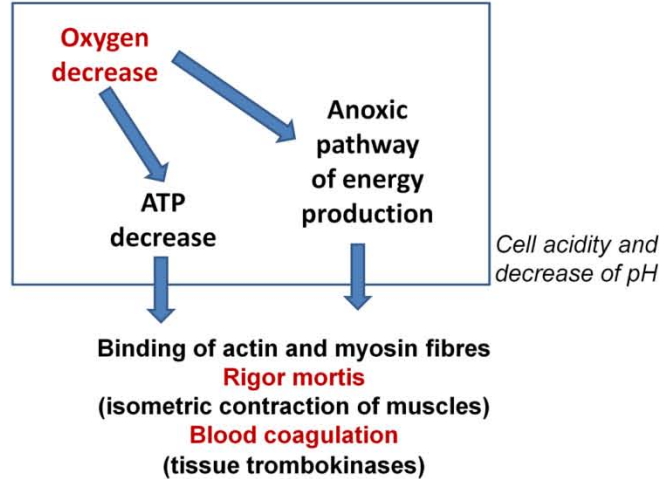


Figure 2. Consequences of the postmortem deoxygenation of blood

2. MATERIALS AND METHODS

Illumination was performed in quad configuration where the linear light sources were placed in both orthogonal and backward mode with approximately twice more energy going into orthogonal mode. We used a custom designed pulsed titanium sapphire laser from Quanta Systems (Solbiate Olona, Italy) operating at 10 Hz repetition rate with center wavelength of 764nm. Energy output through the illumination system was about 1mJ/cm² measured at the location of the subject. Acoustic signals were measured with an arc array of 64 piezo-composite elements (central frequency of 3.1 MHz) spanning a 152° arc angle with a focal length of 65mm (Imasonic SAS, Voray sur l'Ognon, France). Mice were

kept at a constant temperature around 35°C within a PID controlled water tank. A DGM60-ASK Vexta rotational motor and EZ Limo linear motor from Oriental Motors were used to rotate the mouse as well as to control its position along the axis of rotation during scans. Additionally, a Newport manual XY translational stage was added in order to align the rotation axis to pass through the focal point of the arc. The acquisition sampling frequency was set to 25MHz and 1536 samples were collected for each of the 64 channels.¹⁴ A picture of the OA setup with mouse, arc probe, and illumination bars is seen in Figure 3.

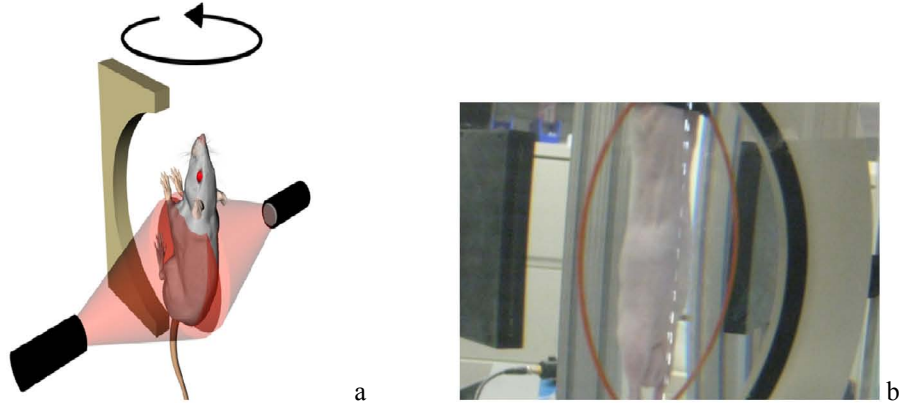


Figure 3. Schematic diagram (a) and a photograph (b) of the LOIS-3D imaging module (within a water tank) with a mouse and the arc probe in the center, and black illumination bars positioned in orthogonal and backward optoacoustic modes.

We used four male Athymic Nude-Foxn1^{nu} mice (Harlan, Indianapolis Indiana) that were 6 to 7 weeks old at the time of the scans. They ranged in body mass from 22 to 26g. Each acquired dataset was averaged 64 times. The rotation was up to 360 degrees with 2.4 degree steps providing a total of 150 data sets and took about 15 minutes. In-vivo mice imaging was done with the use of a mixture of isoflurane and room air that put the mice to sleep and acted as an analgesic. A custom made mouse holder used in our prior studies was used to provide ample imaging area of the body while creating a diving bell for required air.¹⁵ After live OA scans, the mouse was taken out of the water tank still held in the mouse holder and euthanized with potassium chloride while under isoflurane. After verification of death by observing breathing patterns, the mice were placed back into the imaging tank and immediately scanned. The dead mouse would be left in the water tank until a second scan would be taken two hours postmortem to allow for rigor mortis to set. The mouse would then be taken out of the water tank and wrapped in wet towels, then covered with plastic wrap, and placed in a refrigerator at 4-6°C overnight. The dead mouse was taken out of the refrigerator the following day around half hour prior to its next scan and placed back into the OA imaging system to allow for temperature stabilization. The third postmortem scan was done over 20 hours after the euthanasia to see changes caused by rigor mortis and blood coagulation. In this manner, temperature changes should not be significant due to control of the ambient water temperature during scans and allowing the postmortem mice core temperature to stabilize following refrigeration.

Signal processing was kept the same among all the mice involved, using deconvolution of the acousto-electric impulse response, 7-scaled wavelet transform, and a single principal component removal.¹⁶ A full data set from 150 acquisitions spread over 2.4 degrees apart created a sphere of 9600 transducers that could be reconstructed into a volume of 45 million voxels in less than 55 seconds.¹⁷ Image processing was kept constant across all mice such that it was based on percentages associated with their respective histograms of the initial in-vivo images. This would allow for a single mouse to be compared across all postmortem scans as well as give a feeling of how each scan performed with respect to one another. Using Volview 2.0 from Kitware, the scalar opacity mapping forced all negative values up to 0 transparent. Then a linear opacity ramp up was applied up a level of 0.3 at 70% of the dynamic range of the histogram followed by the maximum level of 1 immediately afterwards. Color mapping was done in a similar manner such that blue was set to 0 transitioning to green at 20% the dynamic range of a live scan and becoming flat red at 70%. Gradient opacity mapping was mostly handled such that all lower gradients up to the intensity distribution mode were zeroed out with Volview automatically setting the ramp to match with its Strong Edge detection heuristics.

3. RESULTS & DISCUSSION

Using prior experience with optoacoustic imaging of a live mouse we could predict that blood rich regions would show up well.^{18,19} This was once more the case as we saw similar in quality visualization of the spleen, left and right kidneys, and some major blood vessels like the femoral veins. All these were seen in the in-vivo scans of the mice and the image processing was such that those regions were seen but mainly colored green and yellow as observed in Figure 4. The first set of postmortem scans could also be considered a control scan since it was performed immediately after death of the mouse. There was a definite increase in contrast in the initial postmortem images as compared to in vivo images as more areas of red were found, especially within the spleen, kidneys, and larger blood vessels. Also, the fragments of liver became visible over the right kidney as seen in Figure 5. The belief for the major reason of this enhancement is the loss of movement artifacts due to breathing and blood circulation although deoxygenation would be happening during this time period as well.

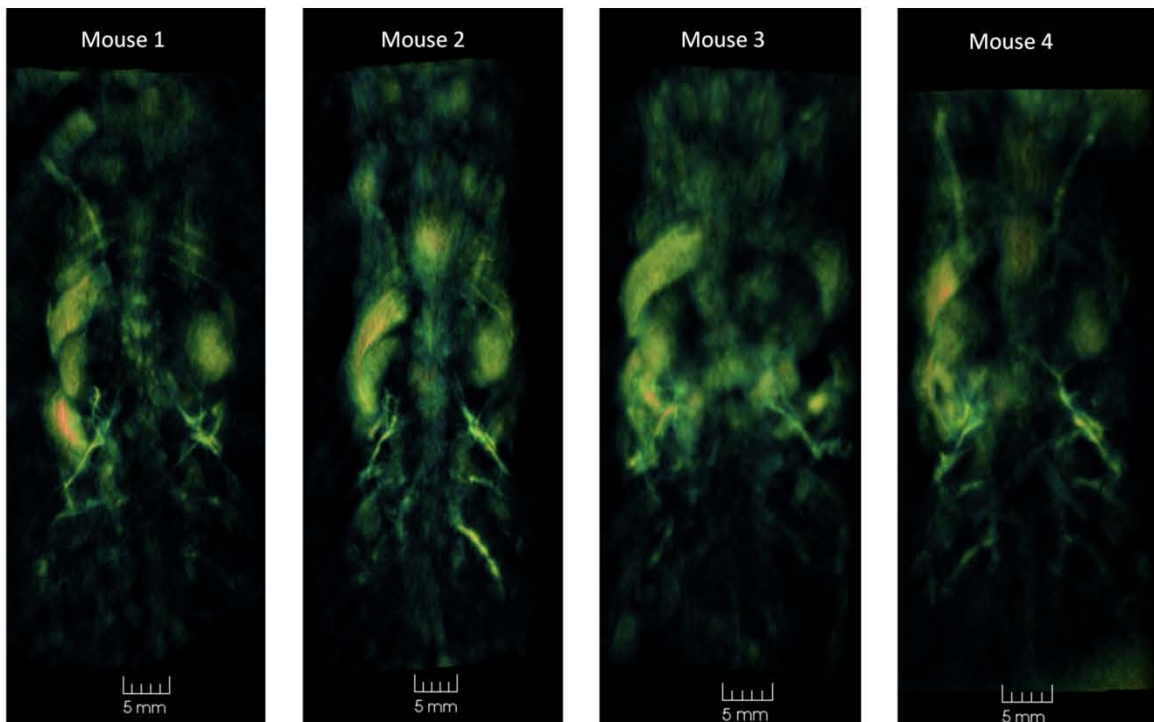


Figure 4. In-vivo OA images of the four mice

The second postmortem scan done two hours after euthanizing showed an even greater increase in contrast than both in-vivo and 5 minutes postmortem which is shown in Figure 5. Comparing the two postmortem scans, this increase would not be due to the loss of breathing but physiological and chemical changes that may occur within that time frame. There is an even higher contrast found within the spleen, kidneys, and larger blood vessels. The liver over the right kidney is becoming more opaque with more regions of red as well. Smaller branching blood vessels are also becoming more apparent during these times, of note are those below the kidneys and near the gonadal veins. At this time, deoxygenation of the blood should be close to finalized but more importantly blood coagulation and rigor mortis should be ongoing. It was noticed that at the end of the scan the mouse was relatively stiff.

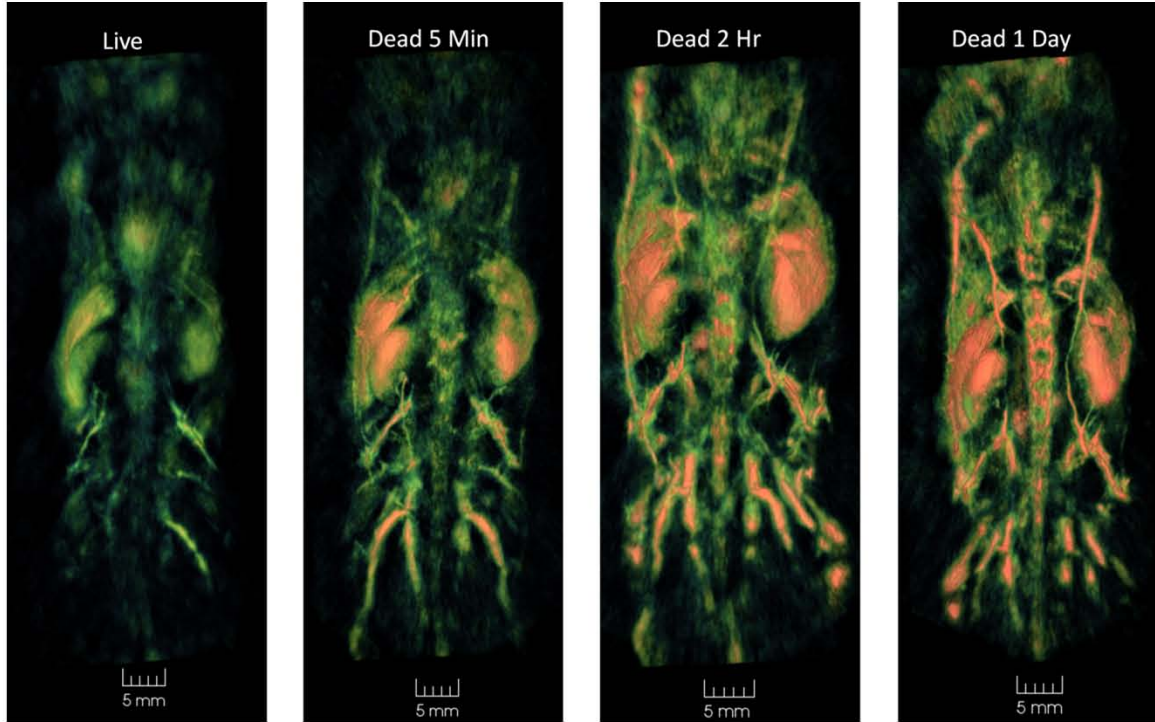


Figure 5. Postmortem changes of optoacoustic images of one of the mice

The last postmortem scan done about a day after euthanizing the mouse once more showed an overall increase in contrast around the targets seen prior in the 2 hour scan. There was also less of a static noise around those contrasted objects of interest as well as organs showing less contrast around their edges as compared to before. Particularly significant increase in the optoacoustic contrast was observed around the vertebrae. This was possibly attributed to more blood coagulation around the vertebrae due to the hemolytic effect of an acidic medium progressing into the later stages. Additionally, it is possible that the advanced stage of rigor mortis further limited any small movements due to rotating in the water. Temperature should not be an issue in our imaging since the acoustically coupling medium is warm water that is maintained at a constant temperature for about thirty minutes prior to the scan to help stabilize the mouse after refrigeration. All these observations can be seen in Figures 4 and 5 which show two of the mice imaged using 764nm wavelength.

With just one wavelength, it is not clear how sensitive the present optoacoustic images are to the deoxygenation of blood. Using titanium sapphire where deoxygenated blood is more absorbing as compared to oxygenated blood, one can infer that it should help increase the contrast further in time from when it was alive but how much is uncertain. There would need to be at least one secondary wavelength where oxygenated blood would be more absorbing like 1064nm, available in a YAG laser. This would help confirm which effects are due to acoustic changes such as rigor mortis and blood coagulation and which are due to optical changes in oxyhemoglobin and deoxyhemoglobin. Another addition to these experiments would be the addition of longer term studies where rigor mortis would begin to alleviate in determining its effect in optoacoustic imaging. This would hypothetically help in determining if our increased contrast was due to blood coagulation alone or if rigor mortis did add some element of increase contrast.

4. CONCLUSION

In this work, we were interested in identifying the changes that could be detected using optoacoustic 3D tomography in dying mammalian organisms. Such an issue may arise from cases like frostbite where a localized cold injury is often found in feet and toes or hands and fingers. If the damage is extensive enough, amputation of the body part is required and possibly using OA imaging one can quickly differentiate regions of dead tissue from live. It was seen here that

within a day there is a general increase in contrast associated with blood rich tissues and organs. It is probably related from a combination of optical changes from blood coagulation and deoxygenated blood as well as acoustic changes from blood coagulation and rigor mortis. Concerning deoxygenated blood though, there is a need to add a scan with a separated laser wavelength preferably something like 1064nm where oxygenated blood absorbs more as opposed to deoxygenated blood seen at 764nm. Also, it would be beneficial to continue scans past a day after an animal's death to see at which point OA imaging starts degrading and its correlation to changes in cadaverous tissue at that time. If optoacoustic imaging can monitor and track all the various blood and tissue related changes in the body it might be used to help estimate the time of death.

ACKNOWLEDGEMENTS

This work was supported in part by grants from the National Cancer Institute (R44CA110137) and The National Institute of Environmental Health Sciences (R43ES021629) The authors thank Travis Hernandez for his technical support of data acquisition.

5. REFERENCES

- [1] Kala M. and Chudzikiewicz E., "The influence of post-mortem changes in biological material on interpretation of toxicological analysis results", *Problems of Forensic Sciences*, 54, 32-59 (2003).
- [2] Estracanholli E.S., Kurachi C., Vicente J.R., Fernanda P., Menezes P.F.C., Silva Júnior O.C., and Bagnato S.V. , "Determination of post-mortem interval using *in situ* tissue optical fluorescence", *Opt. Express* 17 (10), 8185-8192 (2009) .
- [3] Beard P.C., and Mills T.N., "Characterization of *post mortem* arterial tissue using time-resolved photoacoustic spectroscopy at 436, 461 and 532 nm", *Phys. Med. Biol.* 42, 177-198 (1997).
- [4] Maab H. and Kuhnapfel U., "Noninvasive Measurement of Elastic Properties of Living Tissue", 13th Intern. Cong. on Computer Assisted Radiology and Surgery, 865-870 (1999).
- [5] McKenna M.F. Goldbogen J.A., Leger J.S., Hildebrand J.A., and Cranford T.W., "Evaluation of postmortem changes in tissue structure in the bottlenose dolphin (*Tursiops truncatus*)", *The Anatomical Record* 290, 1023–1032 (2007).
- [6] Persson A, Jackowski C, Engström E, and Zachrisson H., "Advances of dual source, dual-energy imaging in postmortem CT", *Eur. J. Radiol.* 68(3), 446-455 (2008).
- [7] Liu Y., Lyon B. G., Windham W. R., Lyon C. E., and Savage E. M., "Principal Component Analysis of Physical, Color, and Sensory Characteristics of Chicken Breasts Deboned at Two, Four, Six, and Twenty-Four Hours Postmortem", *Poultry Science* 83, 101–108 (2004).
- [8] Yarema M.C. and Becker C.E., "Key concepts in postmortem drug redistribution", *Clin. Toxicol.* 43(4), 235-241 (2005).
- [9] Kotz C.M., "Evaluation of a quantitative magnetic resonance imaging system for whole body composition analysis in rodents", *Obesity* 18(8), 1652-1659 (2010).
- [10] Watchman H., Walker G.S., Randeberg L.L., and Langlois N.E.I., "Re-oxygenation of post-mortem lividity by passive diffusion through the skin at low temperature", *Forensic Science, Medicine, and Pathology* 7(4), 333-335 (2011).
- [11] Oraevsky A.A. and Karabutov, A.A., [Biomedical Photonics Handbook], "Optoacoustic Tomography", CRC Press, Boca Raton - London - New York - Washington, DC, 34/31-34/34 (2003).
- [12] Roggan A., Friebel M., Dörschel K., Hahn A. and Müller G., "Optical Properties of Circulating Human Blood in the Wavelength Range 400–2500 nm", *J. Biomed. Opt.* 4 (36), 31-46 (1999).
- [13] Barton, J. K., Frangineas, G., Pummer, H. and Black, J. F., "Cooperative Phenomena in Two-pulse, Two-color Laser Photocoagulation of Cutaneous Blood Vessels", *Photochemistry and Photobiology* 73, 642–650 (2001).
- [14] Brecht H.P., Su R., Fronheiser M., Ermilov S.A., Conjusteau A., and Oraevsky A.A., "Whole Body Three-Dimensional Optoacoustic Tomography System for Small Animals," *J. Biomed. Opt.* 14, 064007 (2009).
- [15] Su R., Liopo A.V., Brecht H. P., Ermilov S.A., Larin K. and Oraevsky A.A., "Optoacoustic tomography in preclinical research: *in vivo* distribution of highly purified PEG-coated gold nanorods," *Proc. of SPIE* 8089, 808902 (2011).
- [16] Wang, K., Ermilov, S.A., Su, R., Brecht, H., Oraevsky, A.A., and Anastasio, M.A., "An Imaging Model

- Incorporating Ultrasonic Transducer Properties for Three-Dimensional Optoacoustic Tomography”, Proceedings of IEEE Trans. Med. Imaging, 203-214 (2011).
- [17] Su R., Brecht H.-P., Ermilov S.A., Nadvoretsky V., Conjusteau A., and Oraevsky A.A., “Towards Functional Imaging using the optoacoustic 3D whole-body tomography system”, Proc. of SPIE 7564, (2010).
- [18] Fronheiser M.P., Stein A., Herzog D., Thompson S., Liopo A., Eghtedari M., Motamedi M., Ermilov S., Conjusteau A., Gharieb R., Lacewell R., Miller T., Mehta K., and Oraevsky A.A., “Optoacoustic System for 3D Functional and Molecular Imaging in Nude Mice”, Proc. of SPIE 6856, (2008).
- [19] Ermilov S.A., Khamapirad T., Conjusteau A., Leonard M.H., Lacewell R., Mehta K., Miller T., and Oraevsky A.A., "Laser optoacoustic imaging system for detection of breast cancer," Journal of biomedical optics 14(2), 024007 (2009).